Journal of Medicinal and Chemical Sciences 7 (2024) 969-982

Journal of Medicinal and Chemical Sciences

Journal homepage: http://www.jmchemsci.com/

Original Article

An Investigation of Atorvastatin Calcium Loaded Transethosomes for Transdermal Delivery and Validation of HPLC Methods

Pramulani Mulya Lestari[1,4], Melva Louisa[2], Yahdiana Harahap[3], Silvia Surini[1,*]

[1]*Laboratory of Pharmaceutics and Pharmaceutical Technology, Faculty of Pharmacy, Universitas Indonesia, Depok, West Java, Indonesia*
[2]*Department of Pharmacology and Therapeutics, Faculty of Medicine, Universitas Indonesia, Jakarta, Indonesia*
[3]*Bioavailability/Bioequivalence Laboratory, Faculty of Pharmacy, Universitas Indonesia, Depok, Indonesia*
[4]*Department of Pharmaceutics, Faculty of Pharmacy and Sciences, Universitas Muhammadiyah Prof. DR. HAMKA, East Jakarta 13460, DKI Jakarta, Indonesia*

ARTICLEINFO

Article history

Received: 2024-05-31
Received in revised: 2024-06-17
Accepted: 2024-07-11
Manuscript ID: JMCS-2405-2527

DOI:10.26655/JMCHEMSCI.2024.7.8

KEYWORDS

Atorvastatin calcium
Transethosomes
Transdermal drug delivery
Validation

ABSTRACT

Atorvastatin calcium is an antihyperlipidemic agent with low bioavailability due to the first-pass metabolism after oral administration. To overcome the limitation, an alternative method for delivering drug molecules to the systemic circulation is needed, such as transethosomes produced for transdermal delivery. Therefore, this study aimed to produce atorvastatin calcium transethosomes with characteristics suitable for transdermal delivery using validated analytical method. Transethosomes formulations were prepared with different concentrations of soy lecithin and ethanol. All formulations were evaluated for particle size, zeta potential, polydispersity index (PDI), drug content, and deformability index. Validation of the analytical method of atorvastatin calcium was carried out using system suitability, selectivity, linearity, limit of detection (LOD), limit of quantification (LOQ), precision, accuracy, and robustness. The result showed that transethosomes had a small particle size of 123.90 nm-165.10 nm, high zeta potential values, acceptable PDI, the highest atorvastatin calcium content, and good deformability index. In addition, the system suitability test results were acceptable and there was no interference in the atorvastatin calcium area. Linearity showed r =0.9999 with LOD and LOQ values of 0.388 µg/mL and 1.176 µg/mL, respectively. The % RSD in the precision was < 2 and the recovery in the accuracy was 98.76%-101.04%. The method proved to be robust with respect to mobile phase pH changes. Based on the results, atorvastatin calcium-loaded transethosomes were suitable for transdermal delivery and could be effectively produced with a 3% soy lecithin and 30% ethanol concentration. The analytical method for determining drug content of atorvastatin calcium-loaded transethosomes could be effectively applied.

* Corresponding author: Silvia Surini
✉ E-mail: silvia@farmasi.ui.ac.id

GRAPHICAL ABSTRACT

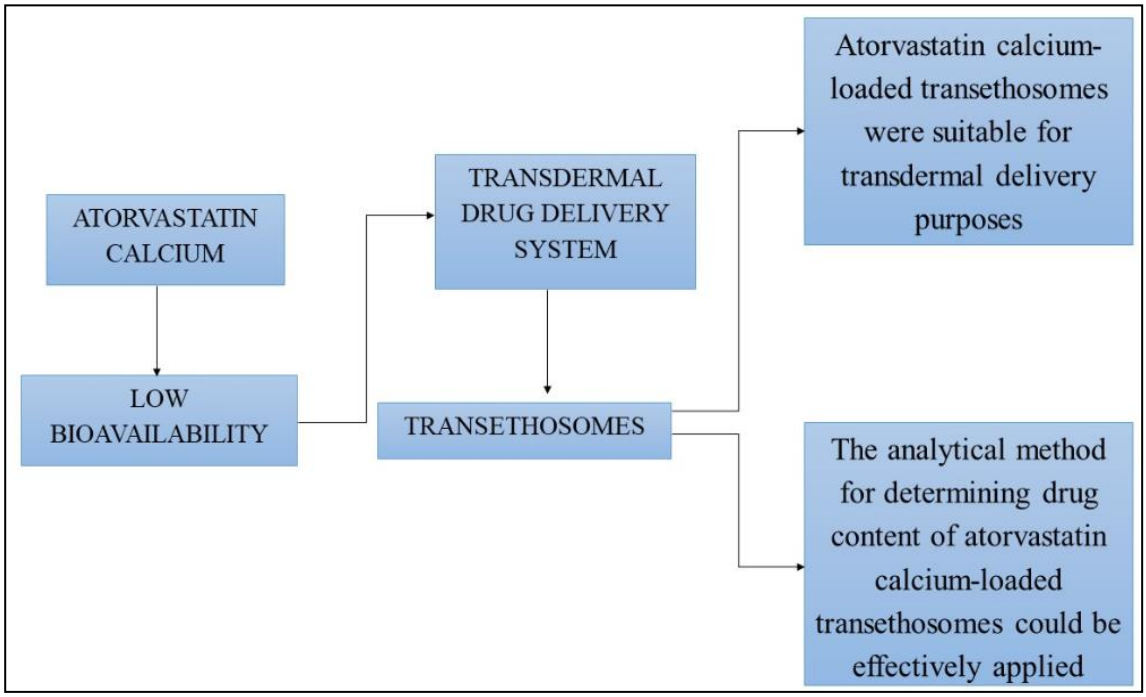

Introduction

Atorvastatin calcium is a drug with low bioavailability and often subjected to intestinal wall extraction through the catalytic activity of the CYP3A4 enzyme. The extraction process has been reported to contribute to apical recycling mediated by intestinal P-glycoprotein or other efflux proteins [1].

In addition, an essential aspect of the process comprises glucuronidation catalyzed by uridine diphosphate glucuronosyltransferase (UGT) 1A1 and 1A3 [2]. To overcome the challenge associated with atorvastatin calcium, several studies recommended the use of transdermal delivery system as an effective method. The method can be used to address low bioavailability by transporting drug compounds through the skin layers into the systemic circulation [3].

This route avoids first-pass metabolism, permitting the drug to enter systemic circulation without encountering obstacles, such as pH, enzymes, or bacteria in the gastrointestinal tract [4]. The development of transdermal delivery system has also been found to increase the bioavailability of several drug types, including the fluvastatin sodium spanlastic nanovesicles can increase bioavailability by 2.79 fold [5], raloxipine encapsulated spanlastic nanogel increses bioavailability 2.15 fold [6] and the bioavailability of the pioglitazone patch increases by 2.2 times compared to the oral route [7]. According to the previous studies, the skin is the largest organ of the body with potential for adequate drug delivery compared to other biological membranes despite the slower permeation rate due to the presence of stratum corneum in the outermost layer [4].

Various strategies have been implemented to increase drug delivery through the skin, including the use of chemical penetration enhancers, physical methods, and vesicular systems. However, penetration enhancers can cause skin irritation and are limited to drug types with small molecular weights. Physical methods, such as iontophoresis, also pose a risk of burns when electrodes are misused [4], while vesicular systems comprising liposomes, transfersomes, ethosomes, and transethosomes are known to be biocompatible and biodegradable [8].

Each of the vesicular systems has been reported to have unique characteristics due to the constituent components, leading to different penetration mechanisms.

For instance, liposomes are composed of cholesterol intercalating between phospholipid molecules to produce rigid vesicles [9]. Transfersomes consist of phospholipids and an edge activator (surfactant), which forms deformable vesicles [9], while ethosomes consist of phospholipids and high ethanol concentrations capable of enhancing drug molecule penetration [10].

In addition, transethosomes are a combination of ethosomes and transfersomes, generating ultradeformable vesicles [11]. The flux value of piroxicam transethosomes is higher than liposomes, transfersomes and ethosomes [12]. In this context, paeonol transethosomes have particle size, polydispersity index (PDI), entrapment efficiency, flux, and AUC values, which are superior to the characteristics of transfersomes [13]. This study selected transethosomes due to the ability to increase penetration through the effect of the ethanol component, thereby, increasing fluidity and decreasing density of the stratum corneum [14]. The procedure was followed by the effect of the ultradeformable transethosomes system, which penetrates through a smaller narrow gaps when compared to the diameter [15]. There has been no previous research in the development of atorvastatin calcium-loaded transethosomes.

Over the years, several methods for assessing atorvastatin calcium have been reported. However, the majority of the methods have focused on determining the drug content in tablet dosage form and in combination with other compounds. This indicates that an analytical technique for determining the active compound atorvastatin calcium content in transethosomes is needed to evaluate the amount of atorvastatin content. According to ICH Q2 (R2) guidelines, quantitative drug compound testing in drug products or other components must use a validated analytical technique to ensure reliable and reproducible results. Therefore, this study aims to produce atorvastatin calcium-loaded transethosomes that meet the required criteria of particle size, zeta potential, drug content, PDI, and deformability index for transdermal delivery system, and obtain a validated analytical method for determining drug content of atorvastatin calcium in transethosomes carriers.

Materials and Methods

The materials used in this study included atorvastatin calcium trihydrate (PT. Kimia Farma Sungwun Pharmacopea, Indonesia), oleic acid (Avantor, USA), soy lecithin (Lecico, Germany), and ethanol (Munggur Putu Karso, Indonesia). Meanwhile, the reagents and solvents of every other type were of analytical grade.

Preparation of Atorvastatin Calcium-Loaded Transethosomes

This study commenced with the preparation of transethosome formulations for atorvastatin calcium, incorporating soy lecithin, oleic acid, and ethanol, as presented in Table 1.

Table 1: Formulations of atorvastatin calcium-loaded transethosome

Formulations	Atorvastatin calcium trihydrate (mg)	Soy lecithin (g)	Oleic acid (mL)	Ethanol (mL)	Distilled water up to
F1	432	1	6	20	100
F2	432	1	6	25	100
F3	432	1	6	30	100
F4	432	3	6	20	100
F5	432	3	6	25	100
F6	432	3	6	30	100
F7	432	5	6	20	100
F8	432	5	6	25	100
F9	432	5	6	30	100

Transethosomes were produced using the method developed by Song *et al.* with slight modifications [16]. Furthermore, atorvastatin calcium was dissolved in oleic acid and ethanol, stirred using a magnetic stirrer at 700 rpm, and followed by the addition of soy lecithin to the mixture. Homogenization was then carried out at 10,000 rpm, and continuously added with distilled water. The resulting transethosomes were filtered using a mini extruder with a 200 nm pore membrane [17], and evaluated.

Particle Size, Zeta Potential, and Polydispersity Index

A particle size analyzer, Anton Paar Letisizer 500, was used for this assessment (Anton Paar, Austria), and the measurements were carried out at room temperature (25 ˚C), with samples initially diluted in distilled water at a ratio of 1:20. This instrument had appropriate software for particle size, polydispersity index (PDI), and zeta potential analysis, while all measurements were conducted in triplicate.

Deformability Index

Vesicles were extruded for 5 minutes through a filter membrane with 100 nm pores in a mini extruder equipped with a vacuum pump. Furthermore, the volume of transethosomes collected in 5 minutes was measured, and the particle size post-extrusion was evaluated with particle size analyzer (Letisizer 500 Anton Paar). Deformability index was calculated using the following equation:

$$D = J\left(\frac{rv}{rp}\right)^2 \qquad (1)$$

Where, D denotes vesicle deformability index, J is the volume of transethosomes passing through the filter membrane in 5 minutes (mL), rv is vesicle size after extrusion (nm), and rp is the membrane pore size (nm).

Validation Method

Chromatographic Conditions

The quantity of atorvastatin calcium loaded in transethosomes system was determined using HPLC (Shimadzu, Japan), with a stationary phase column YMC – Triart C_8 150 x 4.6 mm, 5 µm and a mobile phase consisting of purified water, and acetonitrile (48:52) at pH 3.0 was adjusted with phosphoric acid (H_3PO_4). The implemented flow rate was 1.0 mL/minute at UV wavelength 245 nm, column temperature reached 27 ˚C, and injection volume was 10 µL.

Preparation of Mobile Phase

Purified water and acetonitrile were mixed in a ratio of 48:52 and put in a glass beaker, and then adjusted the pH to 3.0 with H_3PO_4, and stirred using a magnetic stirrer until homogeneous and filtered.

Preparation of Standard Solution

Atorvastatin calcium trihydrate was weighed at 13.5 mg, put into a 25 mL volumetric flask, dissolved, and filled with methanol. A total of 1 mL solution was pipetted into a 20 mL measuring flask, and then the mobile phase was added to the limit mark, and the solution was filtered with 0.2 µm filter paper (concentration = 27 µg/mL).

Preparation of Sample Solution

Atorvastatin calcium transethosomes in a 0.25 mL pipette (1 mL = 4.32 mg atorvastatin calcium trihydrate) were put into a 10 mL volumetric flask, dissolved with methanol to the limit mark, and sonicated for 15 minutes. A pipette of 5 mL solution was done and placed in a 20 mL measuring flask, diluted with the mobile phase to the limit mark. The solution was filtered using a 0.2 µm membrane (concentration = 27 µg/mL).

System Suitability

The standard solution was injected into HPLC system with 6 replicates [18], the response was observed at a wavelength of 245 nm, and relative standard deviation (RSD) was calculated. System suitability test requirements were acceptable when RSD value was ≤ 2% and the theoretical plate number N > 2000 with a tailing factor of no more than 2 [19].

Selectivity

The blank solution (methanol), standard, and sample were injected into HPLC system, and there must be no interference with the atorvastatin calcium chromatogram [20].

Linearity

Linearity could be obtained from the linear regression equation of the calibration curve, and the calibration curve was made with 5 different concentrations 10, 20, 30, 40, and 50 µg/mL, using a mobile phase as a dilute [17,19].

Limit of Detection (LOD) and Limit of Quantitation (LOQ)

LOD and LOQ were calculated based on linear regression from the calibration curve [21]. LOD and LOQ values were calculated based on the following formula:

$$LOD = \frac{3.3 \text{ the standard deviation of the response}}{slope}$$

$$LOQ = \frac{10 \text{ the standard deviation of the response}}{slope}$$

Precision and Accuracy

Accuracy and precision were assessed using a minimum of 9 tests of at least 3 concentration levels (3 concentration levels with 3 replicates each) [22]. Accuracy and precision tests were carried out using the placebo spike method by preparing sample solutions at concentrations of 80%, 100%, and 120% [26,27]. In addition, the absorption was measured in 3 replicates at each concentration, accuracy was reported as % recovery, and precision was reported as the coefficient of variation (RSD) [22].

Robustness

Robustness was carried out based on the effect of pH variations in the mobile phase on the analysis results by injecting the standard solution and sample solution 3 times with a pH variation of 0.2 units [18] using H_3PO_4 in the mobile phase condition, namely with pH 2.8, pH 3, and pH 3.2.

Drug Content

For drug content, one mL transethosomes equivalent to 4.32 mg atorvastatin calcium trihydrate was diluted with methanol until the concentration was 21.6 µg/mL. The sample was injected into HPLC system, and the chromatogram and retention time were recorded.

Results and Discussion

Evaluation of Atorvastatin Calcium-Loaded Transethosomes

Particle Size, Zeta Potential, and Polydispersity Index

Transethosomes particle size distribution was determined using dynamic light scattering (DLS). Suspended particles moved randomly, with speed dependent on size, with smaller particles showing faster movement. Moreover, light scattering caused by the samples was successfully detected and recorded [25]. The particle size data used included the average hydrodynamic diameter, specifically essential for characterizing particles in solution and those coated or subjected to surface modification [26].

All transethosome formulations have particle sizes ranging between 123.90 nm to 165.10 nm, with F4 being the smallest and F2 as the largest, as listed in Table 2.

The results showed all formulations had particle size of less than 210 nm, which was suitable for transdermal delivery [27]. Moreover, smaller vesicle size showed better drug permeation into the skin [28]. The use of ethanol in high concentrations could be responsible for the small particle size observed, as ethanol tends to reduce the thickness of the vesicle membrane [29]. However, increasing ethanol concentration does not correlate with decreasing particle size.

Polydispersity index (PDI) values in Table 2 represented particle size uniformity in atorvastatin calcium-loaded transethosomes, respectively, ranging from 0.163-0.238 with the order F1<F2<F3<F8<F6<F7<F9<F4<F5. The values obtained were acceptable and showed a relatively homogeneous vesicular size distribution. Likewise, size homogeneity and

narrow size distribution were confirmed by values below 0.3. It was reported that PDI greater than 0.5 was a very high value and reflected the diverse and heterogeneous vesicle size distribution [30].

Table 2: Characteristics of atorvastatin calcium-loaded transethosomes

Formulations	Particle size (nm)	PDI	Zeta potential (mV)	Drug content (%)
F1	153.69 ± 3.99	0.163 ± 0.01	-40.97 ± 0.71	98.32 ± 0.10
F2	165.10 ± 3.27	0.187 ± 0.01	-47.13 ± 2.24	97.26 ± 0.04
F3	159.17 ± 0.51	0.195 ± 0.04	-46.33 ± 3.13	99.74 ± 1.40
F4	123.90 ± 1.91	0.233 ± 0.01	-63.20 ± 1.42	101.61 ± 0.01
F5	130.38 ± 3.75	0.238 ± 0.01	-61.23 ± 1.08	100.40 ± 0.02
F6	125.88 ± 3.12	0.204 ± 0.03	-56.30 ± 0.72	103.20 ± 0.90
F7	125.28 ± 3.07	0.210 ± 0.01	-58.90 ± 0.26	97.22 ± 0.06
F8	124.75 ± 1.39	0.198 ± 0.01	-43.60 ± 0.26	98.89 ± 0.17
F9	132.18 ± 4.46	0.224 ± 0.01	-42.30 ± 0.30	97.80 ± 0.11

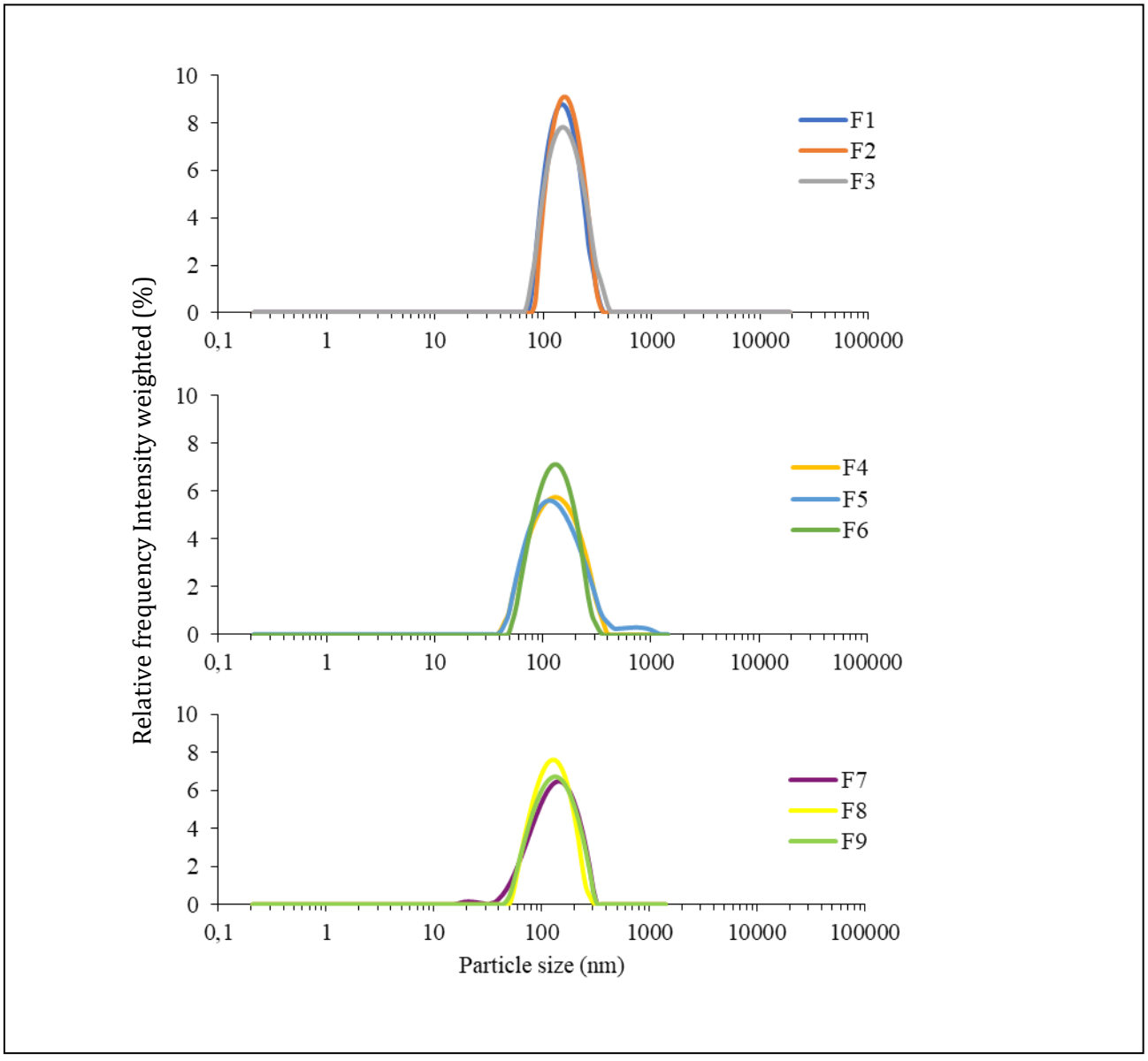

Figure 1: Particle size distribution of atorvastatin calcium transethosomes

The transethosomes particle size distribution of the six formulations was in the range of 16 nm to 1121.4 nm, as displayed in Figure 1. F1 to F3, F4 to F6, and F7 to F9 had a reasonably narrow, fairly wide, and narrow distribution between 71 nm – 400 nm, 40.5 nm – 1121.4 nm, and 16.6 nm – 307 nm, respectively. This showed that F1 to F3 were the most monodispers. This corresponded to the lowest PDI values observed among the most monodispersed formulations including F1 to F3, as presented in Table 2. The particle size distribution provided in Table 3 was calculated based on intensity distribution data and expressed in nm. D_{10} showed that 10% of the total particles had a size smaller than the specified distribution value, while the size of 90% exceeded this value [31]. D_{10} values for atorvastatin calcium-loaded transethosome formulations were in the order F4<F5<F7<F6<F9<F8<F3<F1<F2, respectively, while D_{50} and D_{90} showed that the size of 50% and 90% of the total particles were smaller than the provided distribution value [31]. D_{90} values of all formulations followed the order F8<F6<F9<F7<F1<F4<F2<F3<F5, respectively. All transethosome formulations had a negative (-) charge presented in Table 2 due to the ionization of the phosphate groups of soy lecithin [32] . In addition, ethanol content contributed a negative charge to the polar head groups of phospholipids, which ultimately led to electrostatic repulsion [33,36]. All transethosome formulations containing atorvastatin calcium had zeta potential values ≥ -40.97 mV, presented in Table 2. Zeta potential was measured using electrophoretic light scattering (ELS), which determined the speed of particles in an electric field [25]. Furthermore, it reflected the electrostatic charge on the surface of the lipid bilayer, indicating the stability of the vesicular system [31,37]. Zeta potential values exceeding ± 30 mV indicated good stability [38,39]. In general, with higher zeta potential value, the colloid stability is better [37] and can reduce aggregation [33].

Table 3: The particle size distribution of atorvastatin calcium-loaded transethosomes

Formulations	D10 (nm)	D50 (nm)	D90 (nm)
F1	94.92 ± 1.23	145.36 ± 7.80	224.5 ± 24.98
F2	102.3 ± 1.37	153.14 ± 3.12	232.6 ± 13.21
F3	93.98 ± 6.48	150.17 ± 4.37	249.6 ± 26.59
F4	63.01 ± 2.27	122.07 ± 5.10	231.5 ± 20.65
F5	63.18 ± 1.94	120.16 ± 5.55	277.5 ± 65.39
F6	70.59 ± 3.13	121.39 ± 5.18	204.1 ± 21.87
F7	65.96 ± 3.08	127.33 ± 3.96	219.9 ± 5.75
F8	72.08 ± 0.71	119.82 ± 2.67	194.1 ± 13.93
F9	70.86 ± 3.66	125.58 ± 1.43	216.8 ± 3.67

Drug Content

Transethosomes produced in this study contained 97.22%-103.20% atorvastatin calcium, as presented in Table 2. This indicated uniform distribution of the active ingredient across vesicle and showed that all components were compatible and maintained atorvastatin calcium in transethosomes formulations. Therefore, evaluating the active compound content in formulations was crucial for all dosages, as the content should not significantly differ from the labeled amount, specifically 100 ± 10% [38].

Deformability Index

Vesicle flexibility, a crucial factor for enhancing drug penetration through the skin, was assessed with deformability index data summarized in Table 4. The advantage of transethosomes over other forms of vesicles is their high deformability [39]. Moreover, vesicular systems with good deformability index penetrated lipid membranes without losing integrity [35], and passed through pores smaller than their diameter [15]. In this study, F5 and F6 had a high deformability index and maintained identical size pre and post-extrusion. In addition, increasing ethanol

concentration led to an enhanced deformability index, according to the study by Esposito *et al.* (2022), who showed higher ethanol increased transethosomes vesicle elasticity. A good deformability index resulted from the synergy of oleic acid as a penetration enhancer and ethanol, which interdigitated the lipid bilayer. This interaction promoted vesicle softening and increased deformability index [40]. Therefore, it was effective in delivering atorvastatin calcium through the skin.

Table 4: Deformability index of atorvastatin calcium-loaded transethosomes

Formulations	Particle size before extrusion (nm)	Particle size after extrusion (nm)	Deformability index
F1	153.69 ± 3.99	142.02 ± 3.92	5.05 ± 1.10
F2	165.10 ± 3.27	155.69 ± 2.85	5.68 ± 1.58
F3	159.17 ± 0.51	152.55 ± 3.05	6.18 ± 0.54
F4	123.90 ± 1.91	114.71 ± 9.13	4.96 ± 0.89
F5	130.38 ± 3.75	128.12 ± 3.78	6.7(± 0.35
F6	125.88 ± 3.12	120.89 ± 2.34	6.84 ± 1.01
F7	125.28 ± 3.07	118.31 ± 3.97	4.80 ± 0.48
F8	124.75 ± 1.39	117.27 ± 1.57	5.25 ± 0.92
F9	132.18 ± 4.46	119.92 ± 1.89	6.24 ± 0.60

Validation of Analytical Method

System Suitability

The system suitability test met the requirements, with the percent RSD of the area of re-injection having a value of 0.475% or ≤ 1%, and the theoretical plate number (N) of 6 replicate injections was > 2000 [19]. The greater the N value, the better the column efficiency [19], and the average N value obtained from this study was 50679, described in Table 5. Apart from that, the average value of the tailings factor from 6 injections was 1.062 or no more than 2 [19].

Table 5: System suitability of an analytical method for atorvastatin calcium transethosomes

No.	Area	Theoretical plate number (N)	Tailings factor
1	653542	50397	1.063
2	651915	50775	1.062
3	659412	50669	1.061
4	658859	50668	1.063
5	657874	50798	1.060
6	658230	50767	1.061
Average	656639	50679	1.062
% RSD	0.475%	0.268%	0.104%

Selectivity

Selectivity describes a particular analyte in a matrix that can be measured without interference from other components [18,22]. The results of the standard and sample chromatograms showed that there was no interference with the atorvastatin calcium retention time, as shown in Figure 2. This revealed that the method used was selective for the atorvastatin calcium compound.

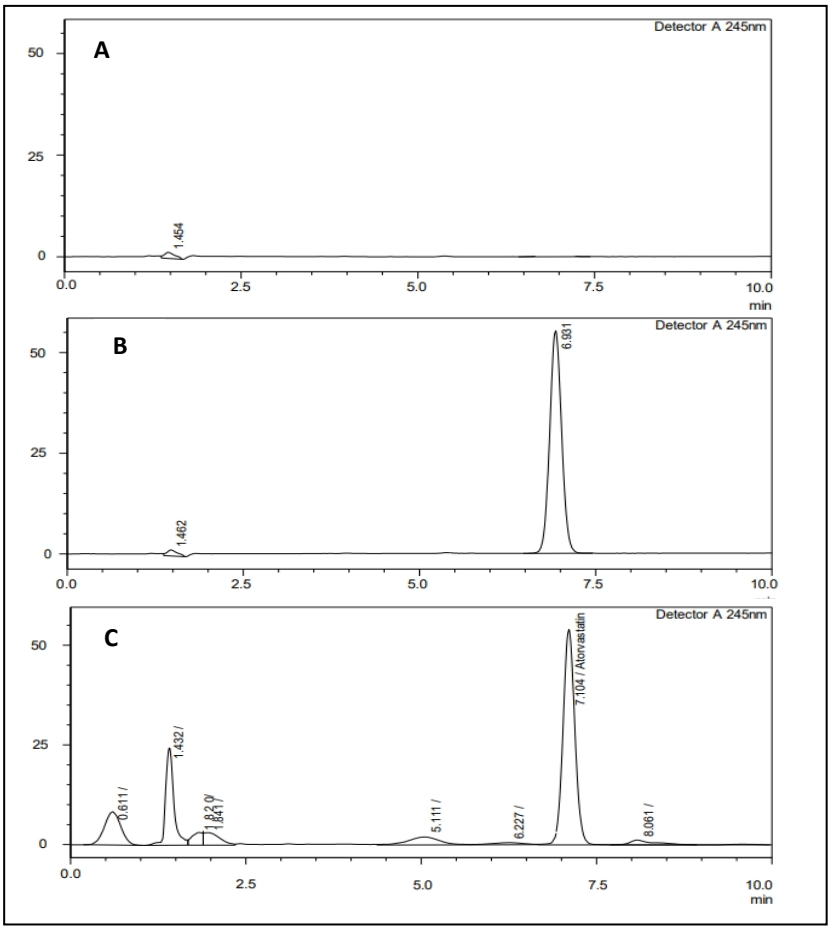

Figure 2: Chromatogram of blank (A), standard (B), and sample (C)

Linearity

Linearity was determined by measurements using 5 concentrations [19], and based on the measurement data, a linear regression line equation (y=a+bx) was created to obtain the correlation coefficient, which showed linearity. The linearity curve in this study showed a correlation coefficient value of r = 0.9999, as demonstrated in Figure 3, which met the requirements, namely r ≥ 0.999 [19].

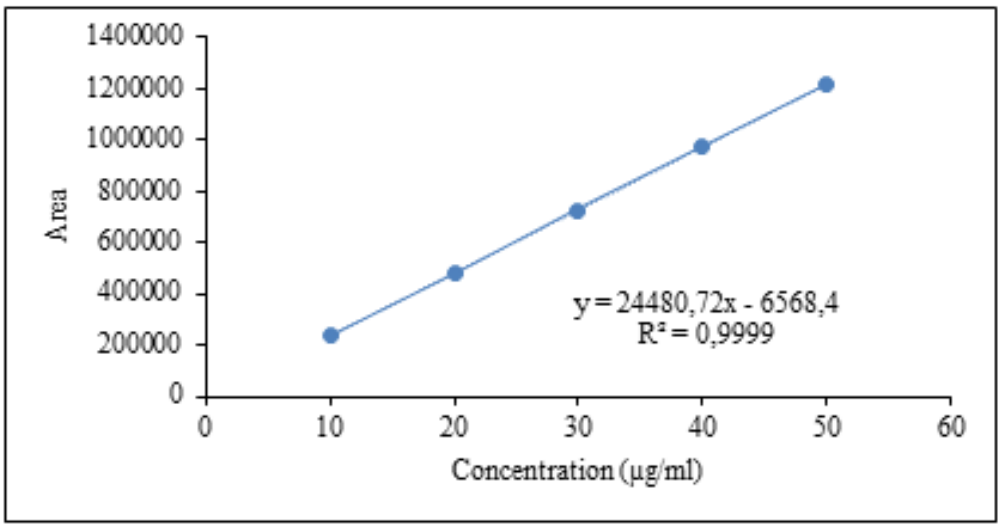

Figure 3: Calibration curve of atorvastatin calcium

Limit of Detection (LOD) and Limit of Quantitation (LOQ)

LOD was the lowest concentration of an analyte in a sample that could be detected, while LOQ was the lowest concentration of an analyte in a sample that was determined with acceptable accuracy and precision under established experimental conditions [21]. LOD and LOQ were calculated based on the calibration curve in Figure 3, so LOD value was 0.388 µg/mL and LOQ 1.176 µg/mL.

Precision and Accuracy

Precision was a measure of the closeness between a series of analyses obtained from several measurements on the same sample. Precision was expressed as the % coefficient of variation of a measurement, and the test results were acceptable according to the requirements for % RSD ≤ 2 [22], at concentrations of 80, 100, and 120%, namely 1.13, 0.66, and 1.08, respectively, as shown in Table 6. Accuracy was a measure that showed the closeness of the analysis result value to the actual analyte level [41]. The test accuracy was expressed in % recovery (98-102%) [41], and the accuracy test in this report met these requirements, namely 98.76%, 101.04%, and 100.54% at concentrations of 80, 100, and 120%, which were presented in Table 6.

Table 6: Precision and accuracy result of an analytical method for atorvastatin calcium transethosomes

Concentration		Recovery		Average of recovery (%)	RSD (%)
µg/mL	%	µg/mL	%		
21.6	80	21.3858	99.0085	98.76	1.13
21.6	80	21.5407	99.7256		
21.6	80	21.0697	97.5449		
27.0	100	27.1152	100.427	101.04	0.66
27.0	100	27.2551	100.945		
27.0	100	27.4704	101.742		
32.4	120	32.1722	99.2968	100.54	1.08
32.4	120	32.7948	101.219		
32.4	120	32.7626	101.119		

Robustness

Robustness was a measure of a procedure's ability to remain viable and not be affected by slight modifications to the procedure [18]. The results of robustness to pH are shown in Table 7, where slight changes in pH with repeated injections of standard solutions and samples produced RSD < 2% were still in acceptable limits [18].

Table 7: Result of robustness of an analytical method for atorvastatin calcium transethosomes

pH	Replication	Standard		Sample	
		Concentration (µg/mL)	RSD (%)	Concentration (µg/mL)	RSD (%)
2.8	1	26.845	0.12	27.144	0.04
	2	26.841		27.168	
	3	26.898		27.156	
3	1	27.210	0.33	27.295	0.15
	2	27.031		27.352	
	3	27.097		27.275	
3.2	1	26.944	0.11	27.341	0.36
	2	26.975		27.197	
	3	26.914		27.153	

Conclusion

To sum up, the results showed that transethosomes containing atorvastatin F6 calcium produced vesicles with a small particle size, namely 125.88 nm. This formulation had an acceptable PDI value for a monodisperse sample and a high zeta potential of -56.2 mV, indicating stability. F6 had the highest drug content of 103.20% and the highest deformability index. Therefore, this formulation was recommended as the most suitable candidate for further study. The analytical method used met the criteria, and it could be used simultaneously in the analysis of determining atorvastatin calcium-loaded transethosomes

Acknowledgements

The authors would like to express their deepest gratitude to the Pharmacy Faculty at the University of Indonesia and the Universitas Muhammadiyah Prof. DR. HAMKA for their invaluable assistance in completing this research endeavor. We are also grateful to the University of Indonesia for providing funding assistance through the PUTI research grant number. NKB-038/UN2.RST/HKP.05.00/2023.

Funding

This research received the PUTI research grant No. NKB-038/UN2.RST/HKP.05.00/2023 from the Directorate of Research and Development of Universitas Indonesia.

Authors' Contributions

All authors contributed to data analysis, drafting, and revising of the paper and agreed to be responsible for all the aspects of this work.

Conflict of Interest

No potential conflict of interest was reported by the authors.

ORCID

Melva Louisa
https://orcid.org/0000-0002-9451-0380
Yahdiana Harahap
https://orcid.org/0000-0002-7217-7900
Silvia Surini
https://orcid.org/0000-0003-1211-9706

References

[1]. Ghim J.L., Phuong N.T.T., Kim M.J., Kim E.J., Song G.S., Ahn S., Shin J.-G., Kim E.Y., Pharmacokinetics of fixed-dose combination of atorvastatin and metformin compared with individual tablets, *Drug Design, Development and Therapy*, 2019, **13**:1623. [Crossref], [Google Scholar], [Publisher]

[2]. a) Lei H.P., Qin M., Cai L.Y., Wu H., Tang L., Liu J.E., Deng C.Y., Liu Y.B., Zhu Q., Li H.P., UGT1A1 rs4148323 A allele is associated with increased 2-hydroxy atorvastatin formation and higher death risk in Chinese patients with coronary artery disease, *Frontiers in Pharmacology*, 2021, **12**:586973. [Crossref], [Google Scholar], [Publisher]; b) Hatefi, M., Komlakh, K., The effect of Atorvastatin on chronic subdural hematoma status: A systematic review of drug therapy, *Journal of Medicinal and Pharmaceutical Chemistry Research*, 2022; **4**:1130. [Pdf], [Publisher]; c) Balavandi, F., Neystani, B., Jamshidbeigi, Y., Mozafri, A., Comparing the effect of drugs atorvastatin and rosuvastatin on the level of laboratory markers acute coronary syndrome patients, *Journal of Medicinal and Pharmaceutical Chemistry Research*, 2022; **4**:894. [Pdf], [Publisher]

[3]. a) Wong W.F., Ang K.P., Sethi G., Looi C.Y., Recent advancement of medical patch for transdermal drug delivery, *Medicina*, 2023, **59**:778. [Crossref], [Google Scholar], [Publisher]; b) Kamali, A., Sofian, M., Mahmodiyeh, B., Valibeik, S., Farahani, E., Effect of atorvastatin on clinical manifestations and outcomes in patients with COVID-19, *Journal of Medicinal and Chemical Sciences*, 2023, **7**:242. [Crossref], [Google Scholar], [Publisher]

[4]. Jeong W.Y., Kwon M., Choi H.E., Kim K.S., Recent advances in transdermal drug delivery systems: A review, *Biomaterials Research*, 2021, **25**:24. [Crossref], [Google Scholar], [Publisher]

[5]. El Menshawe S.F., Nafady M.M., Aboud H.M., Kharshoum R.M., Elkelawy A.M.M.H., Hamad D.S., Transdermal delivery of fluvastatin sodium via

tailored spanlastic nanovesicles: mitigated Freund's adjuvant-induced rheumatoid arthritis in rats through suppressing p38 MAPK signaling pathway, *Drug Delivery*, 2019, **26**:1140. [Crossref], [Google Scholar], [Publisher]

[6]. Ansari M.D., Shafi S., Pandit J., Waheed A., Jahan R.N., Khan I., Vohora D., Jain S., Aqil M., Sultana Y., Raloxifene encapsulated spanlastic nanogel for the prevention of bone fracture risk via transdermal administration: Pharmacokinetic and efficacy study in animal model, *Drug Delivery and Translational Research*, 2023, 1. [Crossref], [Google Scholar], [Publisher]

[7]. Nair A.B., Gupta S., Al-Dhubiab B.E., Jacob S., Shinu P., Shah J., Aly Morsy M., SreeHarsha N., Attimarad M., Venugopala K.N., Effective therapeutic delivery and bioavailability enhancement of pioglitazone using drug in adhesive transdermal patch, *Pharmaceutics*, 2019, **11**:359. [Crossref], [Google Scholar], [Publisher]

[8]. Ahmed T.A., Preparation of transfersomes encapsulating sildenafil aimed for transdermal drug delivery: Plackett–Burman design and characterization, *Journal of Liposome Research*, 2015, **25**:1. [Crossref], [Google Scholar], [Publisher]

[9]. Richard C., Cassel S., Blanzat M., Vesicular systems for dermal and transdermal drug delivery, *RSC Advances*, 2021, **11**:442. [Crossref], [Google Scholar], [Publisher]

[10]. Chauhan N., Vasava P., Khan S.L., Siddiqui F.A., Islam F., Chopra H., Emran T.B., Ethosomes: A novel drug carrier, *Annals of Medicine and Surgery*, 2022, **82**. [Crossref], [Google Scholar], [Publisher]

[11]. Munir M., Zaman M., Waqar M.A., Hameed H., Riaz T., A comprehensive review on transethosomes as a novel vesicular approach for drug delivery through transdermal route, *Journal of Liposome Research*, 2024, **34**:203. [Crossref], [Google Scholar], [Publisher]

[12]. Garg V., Singh H., Bhatia A., Raza K., Singh S.K., Singh B., Beg S., Systematic development of transethosomal gel system of piroxicam: Formulation optimization, in vitro evaluation, and ex vivo assessment, *AAPS PharmSciTech*, 2017, **18**:58. [Crossref], [Google Scholar], [Publisher]

[13]. Chen Z., Li B., Liu T., Wang X., Zhu Y., Wang L., Wang X., Niu X., Xiao Y., Sun Q., Evaluation of paeonol-loaded transethosomes as transdermal delivery carriers, *European Journal of Pharmaceutical Sciences*, 2017, **99**:240. [Crossref], [Google Scholar], [Publisher]

[14]. Mita S.R., Abdassah M., Supratman U., Shiono Y., Rahayu D., Sopyan I., Wilar G., Nanoparticulate system for the transdermal delivery of catechin as an antihypercholesterol: in vitro and in vivo evaluations, *Pharmaceuticals*, 2022, **15**:1142. [Crossref], [Google Scholar], [Publisher]

[15]. Pérez J.V., Cortés D.M.M., y Gómez Y.G., Potential use of transethosomes as a transdermal delivery system for metabolites from Chenopodium murale, *Materials Today Communications*, 2022, **30**:103165. [Crossref], [Google Scholar], [Publisher]

[16]. Song C.K., Balakrishnan P., Shim C.K., Chung S.J., Chong S., Kim D.D., A novel vesicular carrier, transethosome, for enhanced skin delivery of voriconazole: characterization and in vitro/in vivo evaluation, *Colloids and Surfaces B: Biointerfaces*, 2012, **92**:299. [Crossref], [Google Scholar], [Publisher]

[17]. Kumar L., Utreja P., Formulation and characterization of transethosomes for enhanced transdermal delivery of propranolol hydrochloride, *Micro and Nanosystems*, 2020, **12**:38. [Crossref], [Google Scholar], [Publisher]

[18]. Bagal D., Nagar A., Joshi A., Chachare A., Shirkhedkar A., Khadse S., Development and validation of stability-indicating RP-HPLC method for estimation of dalfampridine in bulk drug and tablet dosage form, *Future Journal of Pharmaceutical Sciences*, 2021, **7**:1. [Crossref], [Google Scholar], [Publisher]

[19]. Ravisankar P., Swathi V., Srinivasa Babu P., Shaheem Sultana Md G., Current trends in performance of forced degradation studies and stability indicating studies of drugs, *IOSR Journal of Pharmacy and Biological Sciences*, 2017, **12**:17. [Google Scholar], [Publisher]

[20]. Tiwari A., Bag P., Sarkar M., Chawla V., Chawla P.A., Formulation, validation and evaluation studies on metaxalone and diclofenac potassium topical gel, *Environmental Analysis,*

Health and Toxicology, 2021, **36**. [Crossref], [Google Scholar], [Publisher]
[21]. Omoteso O.A., Milne M., Aucamp M., The validation of a simple, robust, stability-indicating RP-HPLC method for the simultaneous detection of lamivudine, tenofovir disoproxil fumarate, and dolutegravir sodium in bulk material and pharmaceutical formulations, *International Journal of Analytical Chemistry*, 2022, **2022**:3510277. [Crossref], [Google Scholar], [Publisher]
[22]. Maggadani B., Oktaviani E., Harahap Y., Harmita H., Optimization and validation of an analytical method for tranexamic acid in whitening creams by RP HPLC with precolumn derivatization, *International Journal of Applied Pharmaceutics*, 2020, **12**:167. [Crossref], [Google Scholar], [Publisher]
[23]. Astuti E.J., Rafikayanti A., Cahyani D.I., Putri D.B., Comparison of vitamin C analysis using high-performance liquid chromatography versus potentiometric titration, *KnE Medicine*, 2022, 393. [Crossref], [Google Scholar], [Publisher]
[24]. Thakare B., Mittal A., Charde M., Umbarkar R., Kohle N., Chandra P., Kadam M., Development and Validation of Stability-indicating assay UHPLC Method for Simultaneous analysis of Dolutegravir, Lamivudine and Tenofovir disoproxil fumarate in Bulk and Pharmaceutical Formulation, *Research Journal of Pharmacy and Technology*, 2022, **15**:4061. [Crossref], [Google Scholar], [Publisher]
[25]. Gordillo-Galeano A., Mora-Huertas C.E., Hydrodynamic diameter and zeta potential of nanostructured lipid carriers: Emphasizing some parameters for correct measurements, *Colloids and Surfaces A: Physicochemical and Engineering Aspects*, 2021, **620**:126610. [Crossref], [Google Scholar], [Publisher]
[26]. Maguire C.M., Rösslein M., Wick P., Prina-Mello A., Characterisation of particles in solution–a perspective on light scattering and comparative technologies, *Science and Technology of Advanced Materials*, 2018, **19**:732. [Crossref], [Google Scholar], [Publisher]
[27]. Danaei M., Dehghankhold M., Ataei S., Hasanzadeh Davarani F., Javanmard R., Dokhani A., Khorasani S., Mozafari M., Impact of particle size and polydispersity index on the clinical applications of lipidic nanocarrier systems, *Pharmaceutics*, 2018, **10**:57. [Crossref], [Google Scholar], [Publisher]
[28]. Sudhakar K., Mishra V., Jain S., Rompicherla N.C., Malviya N., Tambuwala M.M., Development and evaluation of the effect of ethanol and surfactant in vesicular carriers on Lamivudine permeation through the skin, *International Journal of Pharmaceutics*, 2021, **610**:121226. [Crossref], [Google Scholar], [Publisher]
[29]. Ascenso A., Raposo S., Batista C., Cardoso P., Mendes T., Praça F.G., Bentley M.V.L.B., Simões S., Development, characterization, and skin delivery studies of related ultradeformable vesicles: transfersomes, ethosomes, and transethosomes, *International Journal of Nanomedicine*, 2015, **10**:5837. [Crossref], [Google Scholar], [Publisher]
[30]. Bin Jardan Y.A., Ahad A., Raish M., Al-Jenoobi F.I., Preparation and characterization of transethosome formulation for the enhanced delivery of sinapic acid, *Pharmaceutics*, 2023, **15**:2391. [Crossref], [Google Scholar], [Publisher]
[31]. Gordillo-Galeano A., Mora-Huertas C.E., Hydrodynamic diameter and zeta potential of nanostructured lipid carriers: Emphasizing some parameters for correct measurements, *Colloids and Surfaces A: Physicochemical and Engineering Aspects*, 2021, **620**:126610. [Crossref], [Google Scholar], [Publisher]
[32]. Salem H.F., Kharshoum R.M., Awad S.M., Ahmed Mostafa M., Abou-Taleb H.A., Tailoring of retinyl palmitate-based ethosomal hydrogel as a novel nanoplatform for acne vulgaris management: Fabrication, optimization, and clinical evaluation employing a split-face comparative study, *International Journal of Nanomedicine*, 2021, 4251. [Crossref], [Google Scholar], [Publisher]
[33]. Abdulbaqi I.M., Darwis Y., Assi R.A., Khan N.A.K., Transethosomal gels as carriers for the transdermal delivery of colchicine: Statistical optimization, characterization, and ex vivo evaluation, *Drug Design, Development and Therapy*, 2018, **12**:795. [Crossref], [Google Scholar], [Publisher]
[34]. Kaul S., Jain N., Nagaich U., Ultra deformable vesicles for boosting transdermal delivery of 2-arylpropionic acid class drug for management of musculoskeletal pain, *Journal of Pharmaceutical*

Investigation, 2022, **52**:217. [Crossref], [Google Scholar], [Publisher]
[35]. Surini S., Leonyza A., Suh C.W., Formulation and in vitro penetration study of recombinant human epidermal growth factor-loaded transfersomal emulgel, *Advanced Pharmaceutical Bulletin*, 2020, **10**:586. [Crossref], [Google Scholar], [Publisher]
[36]. Németh Z., Csóka I., Semnani Jazani R., Sipos B., Haspel H., Kozma G., Kónya Z., Dobó D.G., Quality by design-driven zeta potential optimisation study of liposomes with charge imparting membrane additives, *Pharmaceutics*, 2022, **14**:1798. [Crossref], [Google Scholar], [Publisher]
[37]. Lukhele B.S., Bassey K., Witika B.A., The utilization of plant-material-loaded vesicular drug delivery systems in the management of pulmonary diseases, *Current Issues in Molecular Biology*, 2023, **45**:9985. [Crossref], [Google Scholar], [Publisher]
[38]. Abdallah M.H., Elghamry H.A., Khalifa N.E., Khojali W.M., Khafagy E.-S., Shawky S., El-Horany H.E.-S., El-Housiny S., Development and optimization of erythromycin loaded transethosomes cinnamon oil based emulgel for antimicrobial efficiency, *Gels*, 2023, **9**:137. [Crossref], [Google Scholar], [Publisher]
[39]. Aprianti I., Setiawan H., Diflunisal transethosomes for transdermal delivery: Formulation and characterization, *International Journal of Applied Pharmaceutics*, 2023, **15**:61. [Crossref], [Google Scholar], [Publisher]
[40]. Mahmoud D.B., ElMeshad A.N., Fadel M., Tawfik A., Ramez S.A. Photodynamic therapy fortified with topical oleyl alcohol-based transethosomal 8-methoxypsoralen for ameliorating vitiligo: Optimization and clinical study, *International Journal of Pharmaceutics*, 2022, **614**:121459. [Crossref], [Google Scholar], [Publisher]
[41]. Pebriana R.B., Damayanti O., Agustin Y.D., Lukitaningsih E., Bestari A.N., Validation of a high-performance liquid chromatographic method for the assay and dissolution of captopril in mucoadhesive tablet formulation, *Journal of Applied Pharmaceutical Science*, 2021, **11**:066. [Crossref], [Google Scholar], [Publisher]

HOW TO CITE THIS ARTICLE
P.M. Lestari, M. Louisa, Y. Harahap, S. Surini, An Investigation of Atorvastatin Calcium Loaded Transethosomes for Transdermal Delivery and Validation of HPLC Methods. *J. Med. Chem. Sci.*, 2024 7(7) 969-982
DOI: https://doi.org/10.26655/JMCHEMSCI.2024.7.8
URL: https://www.jmchemsci.com/article_200537.html